**JAST**, Vol. 10, No. 2, pp. 37- 47


JAST
Journal of Aerospace Science and Technology

# Optimization of Moving Wingin Ground Effect using Response Surface Method

**A. Esmaeili[1], M. H. Djavareshkian[2*] and A. Parsania[3]**

1, 2. Department of Engineering, Ferdowsi University of Mashhad

3. Department of Engineering, Payame Noor University, Shiraz

[*]Postal Code: 9177948944, Mashhad, IRAN

**javareshkian@ferdowsi.um.ac.ir**

*Optimization of the sectional wing in ground effect (WIG) has been studied using ahigh order numerical procedure and response surface method (RSM). Initially, the effects of the ground clearance, angle of attack, thickness, and camber of wing have been investigated by a high-resolutionscheme, which is highlystrong and accurate. In the numerical simulation, Normalized Variable Diagram (NVD) scheme is applied to the boundedness criteria. In the optimization process, lift to drag ratio (L/D) is considered as an objective function and static conditions and shape parameters are noticeable to be considered as design variables;.Ths is because the main factor in the design of WIG vehicles is moving near the ground and the distance to the ground draws attention to the significance of it.Therefore, the static conditions strenuously defend this view that they are irrefutable parameters in the aerodynamic optimization of WIG vehicles. Adaptive Neuro-Fuzzy Interface System (ANFIS) is employed to generate the surface response, because the objective function and constraints are particularlynoisy. Sensitivity analysis is also done and the sensitivity amount of the objective function from design variables is explored.*

**Keywords:** Ground effect, Wing shape, Response surface, Static condition**,** Optimization

## Nomenclature

| | |
|---|---|
| *PSO* | Particle Swarm Optimization |
| *NVD* | Normalized Variable Diagram |
| *CFD* | Computational Fluid Dynamic |
| $k$ | Turbulence Model Parameter |
| $\varepsilon$ | Turbulence Model Parameter |
| $L$ | Lift Force |
| $D$ | Drag Force |
| $CL$ | Lift Coefficient |
| $CD$ | Drag Coefficient |
| $h$ | Ground Clearance |
| $c$ | Cord Length |
| $AOA$ | Angle of Attack |
| $WIG$ | Wing in Ground |
| $\rho$ | Density |
| $\mu$ | Dynamic Viscosity |
| $t$ | Time |
| $\vec{V}$ | Velocity Vector |
| $\vec{S}$ | Source Term |
| $\vec{T}$ | Stress Tensor |
| $\phi$ | Scalar Quantity |
| $\vec{q}$ | Scalar Flux Vector |
| $SBIC$ | Second and Blending Interpolation Combined |
| $\Gamma$ | Diffusivity Coefficient |
| $I^c$ | Convection Flux |
| $I^D$ | Diffusion Flux |
| $\delta v$ | Cell Volume |
| $F$ | Mass Flux |
| $A$ | Cell Face Area |
| $\bar{x}$ | Normalized Coordinate |
| $\mathcal{K}$ | SBIC Parameter |
| $a$ | convection-diffusion coefficient |
| $Ca$ | Camber |
| $P$ | Pressure |

1. M. Sc.
2. Associat Professor (Corresponding author)
3. M.Sc.

| | |
|---|---|
| *ANN* | Artificial Neural Network |
| *gbest* | Global Best Position |
| *pbest* | Particle best Position |
| *2D* | Two Dimension |
| $\omega$ | weighting function |
| *R* | random function |
| *s* | Position of Particle |
| *m* | Iteration Number |
| *dv* | Displacement due to new Velocity |
| *Re* | Reynolds Number |
| *SIMPLE* | Semi-Implicit Method For Pressure – Linked Equation |
| $S'_\phi$ | Source Term from non-orthogonality, numerical dissipation terms and external sources |

## Introduction

Ground effect vehicles which operate close to the ground by the use of aerodynamic interaction between the wings and the surface known as ground effect,have been the center of researchers' attention for a long time since 1995 [1-13]. The interaction enhances the lift and decreasesthe drag considerably as comparedto an out of ground effect vehicle. Thus, the aerodynamic enhancement promotes the efficiency of the ground effect vehicles against other transportation systems.Therefore, aerodynamicists have sought to make use of some approaches amplifying the device efficiency. One of these approaches is aerodynamic shape optimization based on computational fluid dynamics (CFD). The optimal design of WIG airfoils has been studied by only a few researchers, whereas most of them have focused on the shape geometries. Kim and Joh[14]have obtained the optimized airfoil shape by using the single-objective optimization technology; and Kim and Chun [15] have also performed computational optimization for an airfoil geometry. More recently, Park and Lee [16] have numerically performed an optimization by considering the lift coefficient, static height stability, and lift-to-drag ratio as objective functions and optimized the airfoil structureby a multi-objective optimization algorithm. Furthermore, the optimization ofwing in ground effect has been performed by Lee and Lee [17] and in parallel,finding the optimum shape usingmulti-objective genetic algorithm and the analysis of the three-dimensional wings in ground effect have been carried out by Lee et al. [18, 19]. Another optimization design of an airfoil which moves close to the ground has been investigated by Kim et al. [20], taking into account the device shape based on lift coefficient maximization. In 2013, an aerodynamic shape optimization of WIG vehicle was conducted by three objective functions, lift coefficient, the aerodynamic center of height, and the lift-to-drag ratio [21].

As a result of literature study, these types of designs impose high costs and lose the WIG vehicle advantages while finding the best wing for WIG vehicles remains a great challenge among the researchers. At present, most of the WIG vehicles utilizepredefined static conditions such as angle of attack and ground clearance. Besides, these parameters play a central role in the device efficiency and they are irrefutable variables in the aerodynamic optimization of WIG vehicles which were neglected in the most previous studies.

The aim of the current study is to optimize the shape and static conditions of a sectional wing, moving near the ground. Aiming to achieve this goal, a highly accurate numerical simulation method and response surface methodology (RSM) are designed and the Adaptive Neuro-Fuzzy Interface System (ANFIS) is employed in order to dampthe noise and find the design point perfectly near the global optimum.Theinfluence of design variables, ground clearance, incidence angle, thickness and camber of the foil, have been initially investigated by a high resolution Normalized Variable Diagram (NVD) scheme, used in the boundedness criteria. In the optimization process, lift to drag ratio (L/D) is considered as the objective function and the design variables consist of thickness and camber of airfoil, angle of attack and ground clearance. Subsequently, sensitivity analysis is done and the amount of objective function allergy from design variables is also explored.

## Governing Equation and Discretization

The basic equations, which describe conservation of mass, momentum and scalar quantities can be expressed in the following vector form which is independentfromthe coordinate system.

$$\frac{\delta\rho}{\delta t} + div\left(\rho\vec{V}\right) = S_m \quad (1)$$

$$\frac{\delta(\rho\vec{V})}{\delta t} + div\left(\rho\vec{V}\otimes\vec{V} - \vec{T}\right) = \vec{S}_v \quad (2)$$

$$\frac{\delta(\rho\phi)}{\delta t} + div\left(\rho\vec{V}\phi - \vec{q}\right) = \vec{S}_\phi \quad (3)$$

The stress tensor and scalar flux vector are usually expressed in terms of basic dependent variables. The stress tensor for a Newtonian fluid is:

$$\vec{T} = -P\vec{I} \quad (4)$$

and the Fourier-type law usually gives the scalar flux vector:

$$\vec{q} = \Gamma_\phi grad\phi \quad (5)$$

In this study, $k-\varepsilon$ model is used for turbulence flow. The model is simple and enjoysgood stability with easy convergence.

The discretization of the differential equations is carried out using a finite-volume approachandutilizing the Gaussian theorem. The discrete expressions are presented to refer to only one face of the control volume, namely, e, for the sake of brevity. For any ϕ variable (which may also stand for the velocity components), the result of the integration yields:

$$\frac{\delta v}{\delta t}\left[(\rho\phi)_p^{n+1} - (\rho\phi)_p^n\right] + I_e - I_w + I_n - I_s = S_\phi \delta v \quad (6)$$

WhereI's are the combined cell-face convection $I^c$and diffusion $I^D$fluxes. The diffusion flux is approximated by central differences. The discretization of the convective flux requires special attention and it helps developing the various schemes. A representation of the convective flux for cell-face (e) is:

$$I_e^c = (\rho.V.A)_e\phi_e = F_e\phi_e \quad (7)$$

The value of $\phi_e$is not known and it should be estimated from the values at neighboring grid points by interpolation. The expression for $\phi_e$is determined by the SBIC scheme [22], that is based on the NVD technique [23] using interpolation from the nodes E, P and W. The functional relationship utilized in SBIC scheme for $\bar{\phi}_e$ is given as:

$$\bar{\phi}_e = \bar{\phi}_p,\ IF\bar{\phi}_p \notin [0,1] \quad (8)$$
$$\bar{\phi}_e = -\frac{\bar{x}_p - \bar{x}_e}{\mathcal{K}(\bar{x}_p - 1)}\bar{\phi}_p^{\,2} + \left(1 + \frac{\bar{x}_p - \bar{x}_e}{\mathcal{K}(\bar{x}_p - 1)}\right)\bar{\phi}_p,\ IF\bar{\phi}_p \in [0, \mathcal{K}]$$
$$\bar{\phi}_e = \frac{\bar{x}_p - \bar{x}_e}{\bar{x}_p - 1} + \frac{\bar{x}_p - \bar{x}_e}{\bar{x}_p - 1}\bar{\phi}_p,\ IF\bar{\phi}_p \in [\mathcal{K}, 1]$$

Where

$$\bar{\phi}_p = \frac{\phi_p - \phi_W}{\phi_E - \phi_W}, \qquad \bar{\phi}_e = \frac{\phi_e - \phi_W}{\phi_E - \phi_W} \quad (9)$$
$$\bar{x}_p = \frac{x_p - x_W}{x_E - x_W}, \qquad \bar{\phi}_e = \frac{x_e - x_W}{x_E - x_W}$$

The limits on the selection of $\mathcal{K}$ could be determined in the following way. Obviously, the lower limit is $\mathcal{K} = 0$, which would represent switching between upwind and central differencing. It is not favorable, because it is essential to avoid the abrupt switching between the schemes in order to achieve the converged solution. The value of $\mathcal{K}$ should be kept as low as possible in order to attain the maximum resolution of the scheme. The final form of the discretized equation from each approximation is given as:

$$a_p.\phi_p = \sum_{m=E,W,N,S} a_m.\phi_m + S'_\phi + S_{dc} \quad (10)$$

Where a's are the convection-diffusion coefficients. The term $S'_\phi$ in Eq. (10) contains quantities arising from non-orthogonality, numerical dissipation terms and external sources. For the momentum equations, it is easy to separate the pressure-gradient source from the convection momentum fluxes. $S_{dc}$is the contribution due to the adapted deferred correction procedure.

## RSM Algorithm

This approach is an approximation-based optimization method which is capable offinding good solutions for intricate engineering optimization problems by computing specific values of the objective function for different combinations of the design variables[24, 25]. Indeed, this method has been successfully applied for solving complex engineering problems[26-28]. The main argument to all these problems is the fact that inherent merit functions generally involve both intensive and expensive numerical or experimental tests. However, the number of tests required for the optimization process should be minimized. This method consists of numerical methods in which all design variables are discretized either according to a simple parametric scheme or using a given numerical planning, such as factorial design, orthogonal design, or central composite design[29]. After acquiring data, it is necessary to fit a mathematical equation to describe the behavior of the response according to the levels of values studied.The importance of adopted fitting model is in using an accurate method, Adaptive Neuro-Fuzzy Interface System (ANFIS) [30].Once the surface response is available, conventional optimization techniques, such as gradient-based techniques or global optimization techniques, may be applied to estimate the function optimal point by searching in the constructed surface. In the present study, active-set methodology is employedto find the optimal point and KKT (Karush-Kuhn-Tucker) condition.Also Quasi-Newton algorithms are utilized. The accuracy of the obtained optimal value naturally depends on the selected design and the adopted fitting model[30]. The remaining steps of the RSM-based optimization methodology are aimedto improve the quality of the obtained optimal solutions. Additional numerical tests are performed in orderto acquire additional response surfaces until a convergence criterion is satisfied. If the difference between the optimum values obtained from the surface response and the values obtained via the numerical simulation reaches a given threshold, the optimization process is stopped.The flowchart of the process is depicted in Fig.1.

The objective function for maximizing the lift to drag ratio and design variables, being considered here, consist of the thickness (t/c), camber (Ca/c) of wing section, angle of attack (AOA), and distance from the ground(h/c). The study of the related bibliography allows the designer to define the following interest area: [t/cmin-t/cmax][Ca/cmin-Ca/cmax][AOAmin-

AOAmax][h/cmin-h/cmax]=[0.09-0.15][0-0.04][2.5-7.5][0.1-0.8]. A balanced multilevel design is primarily matriculated with 3 levels for each factor and the numerical simulationis performedfor all levels.

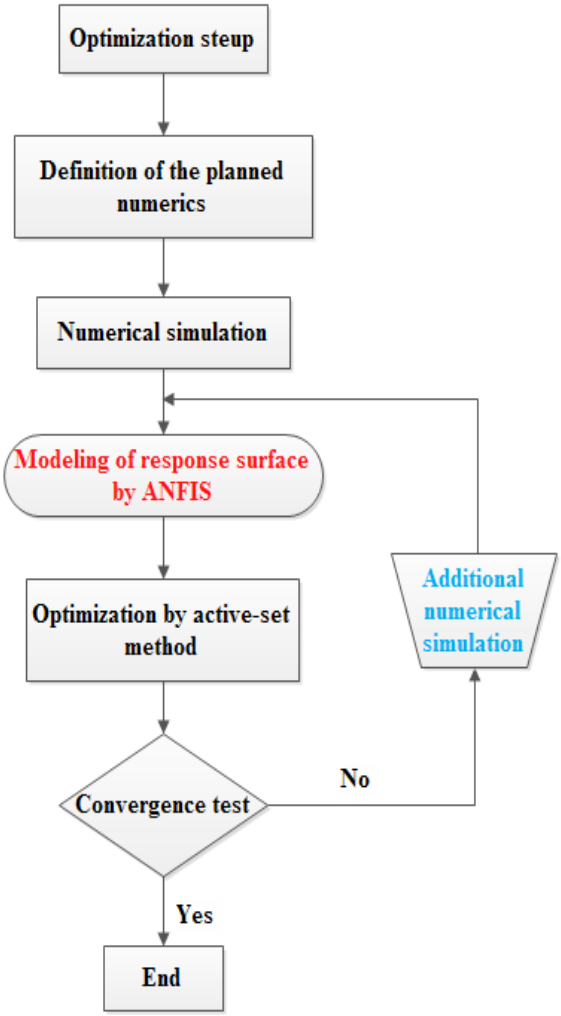


**Figure 1.** Flow chart of RSM method

## Results and Discusion

### Grid generation and validation

In the numerical simulation, grid and domain independency and comparison of the current result with thepublished results data should be investigated. The grid structure that is used in CFD simulation is created by a structured mesh employed because of its simplicity and applicability to the current flow configuration (i.e., with a near-by ground). Schematic shape of these two-dimensional structured grids is illustratedin Fig. 2(a). According to Fig. 2(b), the dimension of domain has been obtained after doing several various lengths for b, f, u and independent lengths have been chosen.

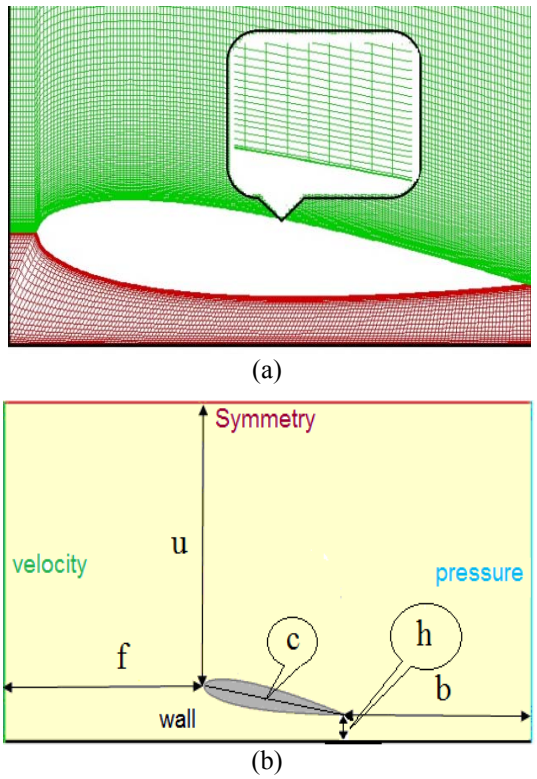


**Figure 2.** (a) H grid topology and H grid. (b) Dimension and boundary condition of 2D domain

The grid sizing is determined after grid independence whichis found by doing several different trials.which illustrate thesurface pressure coefficient distribution. For example, the effect of grid size is exposed in Fig. 3. For other cases, the above process is utilized for grid and domain independences. The setting of numerical simulation are shown in Table 1. The Reynolds number in this study is $2.4\times10^5$.

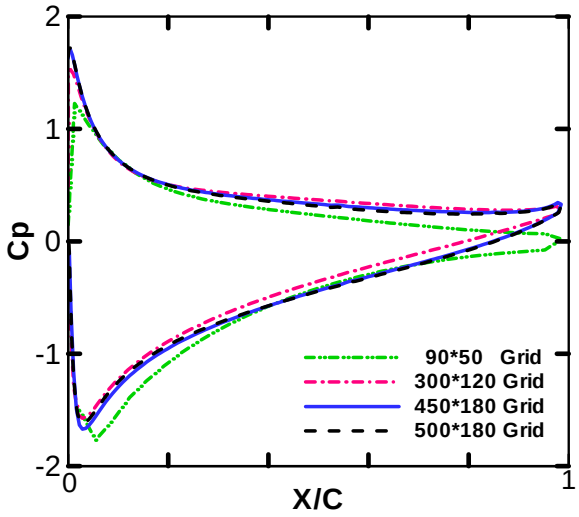


**Figure 3.** Effect of grid sizing on pressure distribution on the surface of the airfoil for10˚ and h/c=0.2angle of attack

**Table 1.** Settings for Numerical Simulation.

| | |
|---|---|
| Flow | turbulent |
| Solver | 2D Double Precision |
| Momentum Equation Solver | Normalize variable diagram |
| Algorithm | SIMPLE |
| turbulent model | $k-\varepsilon$ |
| Bounded scheme | SBIC |

In Fig. 4, the pressure distribution on the surface of NACA0015 airfoil moving near the ground is indicated and validated with experimental data [1]. Figs. 5.a and 5.b demonstrate the velocity profile behind the airfoil at x/c=0.5 and x/c=1 from trailing edge for AOA=5° and h/c=0.1,thenthese results are compared with the experimental data [1]. These comparisons prove the numerical results are in a good argument with experimental data.

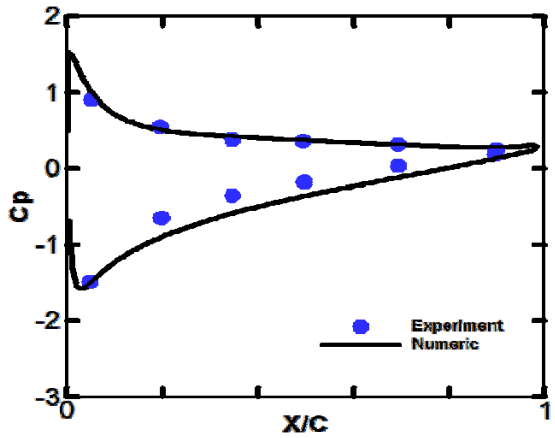


**Figure 4.** Comparison between the present numerical results with experimental data, (a) Pressure coefficient distribution for airfoil NACA 0015 for an AOA 10º and h/c=0.2,

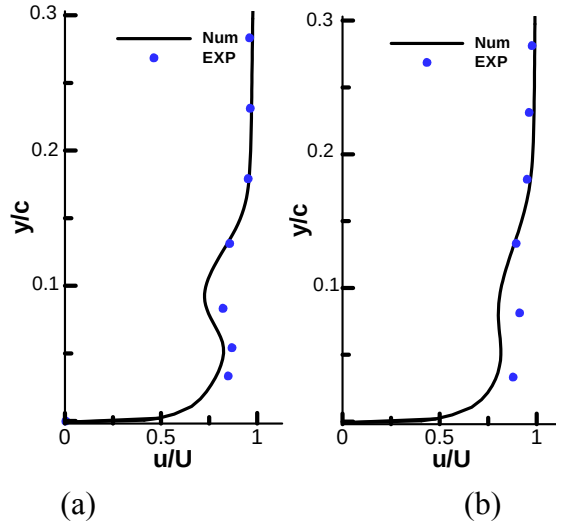


**Figure 5.** Distributions of mean velocity in the wake region of the airfoil for AOA=5˚,h/c=0.1 (a) x/c=0.5 and (b) x/c=1

Subsequently, Table 2 draws an analogy between the lift and drag coefficients for the present numerical results and the experimental data [1] and it can be concluded that the numerical results arehighly congruent with the experimental data. It is noteworthy that the difference between drag coefficients from the numerical simulation and the experiment data is attributed to the airfoil configuration near the ground, turbulent models and the amount of uncertainty in the experimental procedures. Furthermore, the same behaviors are observed in some related publication such as [32],where all of cases in this research are under the same conditions.

**Table 2.** Comparison of the experimental and current numerical aerodynamic coefficients of airfoil NACA 0015 at AOA=2.5°.

| | | CL | CD |
|---|---|---|---|
| h/c=0.1 | Experimental data | 0.370 | 0.0112 |
| | Numerical data | 0.368 | 0.0178 |
| h/c=0.5 | Experimental data | 0.297 | 0.0115 |
| | Numerical data | 0.275 | 0.0220 |
| h/c=0.8 | Experimental data | 0.261 | 0.0118 |
| | Numerical data | 0.265 | 0.0230 |

**Numerical simulation results**

In this research, the e ffect of the camber and thickness of the airfoil have beennumerically investigated in ground proximately for different angles of attack and ground clearances. However, the lift and drag coefficients and lift to drag ratio have been initiallyanalyzed at 3 levels for each factor withspecial angles of attack: 2.5˚, 5˚ and 7.5˚ degrees.Moreover, the ground clearance in this study is fallen into 3 main categories: h/c=0.1, 0.5 and 0.8. Besides, toattain the best airfoil in thepresent condition, the camber and thickness of airfoils were to be taken into consideration; therefore, a broad range of them have beendesignated and both of these parametershave beendivided into 3 segments. The aerodynamic characteristics of these five different 2D airfoils have beeninitially examined according to the assumed cambers and thicknesses. Tables 3(a)-(e) represent the lift and drag coefficients and L/D in thevariant angles of attack as varying ground clearances. In fact, the tables demonstrate some significant trends; for instance, the lift has an upward trend for all cases when the airfoils closely approach the ground. In almost all of the cases, the lift coefficients are dramatically risen by a gradual growth of the camber contrast a slight drop of the thickness. Actually, this behavior lays emphasis on the flow blockage, which hashappened.

Furthermore, drag has the same trend with lift when the ground clearance is slightly changed; whilethis behavior is in agreement with the experimental data [9,11]. On the other hand, this simulation confirms that the drag coefficient in thin airfoils is reduced consistently down from AOA= 2.5°to 5°, after that there is a tendency to rise and the drag tends upward toAOA=7.5°.

**Table 3.** Lift and drag coefficients of the mentioned airfoils

| h/c | 0.1 | | 0.5 | | 0.8 | |
|---|---|---|---|---|---|---|
| AOA (deg) | CL | CD | CL | CD | CL | CD |
| 2.5° | 0.322 | 0.0123 | 0.312 | 0.0130 | 0.298 | 0.0142 |
| 5° | 0.680 | 0.0192 | 0.556 | 0.0222 | 0.539 | 0.0224 |
| 7.5° | 0.890 | 0.0398 | 0.775 | 0.0390 | 0.753 | 0.0405 |

(a) t/c=0.09

| h/c | 0.1 | | 0.5 | | 0.8 | |
|---|---|---|---|---|---|---|
| AOA(deg) | CL | CD | CL | CD | CL | CD |
| 2.5° | 0.315 | 0.0140 | 0.308 | 0.0175 | 0.295 | 0.0180 |
| 5° | 0.645 | 0.0220 | 0.555 | 0.0230 | 0.535 | 0.0256 |
| 7.5° | 0.860 | 0.0350 | 0.765 | 0.0380 | 0.743 | 0.0395 |

(b) t/c=0.12

| h/c | 0.1 | | 0.5 | | 0.8 | |
|---|---|---|---|---|---|---|
| AOA(deg) | CL | CD | CL | CD | CL | CD |
| 2.5° | 0.368 | 0.0178 | 0.275 | 0.0220 | 0.265 | 0.0230 |
| 5° | 0.600 | 0.0230 | 0.550 | 0.0235 | 0.520 | 0.0290 |
| 7.5° | 0.803 | 0.0335 | 0.740 | 0.0340 | 0.730 | 0.0380 |

t/c=0.15

| h/c | 0.1 | | 0.5 | | 0.8 | |
|---|---|---|---|---|---|---|
| AOA(deg) | CL | CD | CL | CD | CL | CD |
| 2.5° | 0.545 | 0.0182 | 0.446 | 0.0265 | 0.429 | 0.0280 |
| 5° | 0.777 | 0.0271 | 0.683 | 0.0289 | 0.661 | 0.0324 |
| 7.5° | 0.987 | 0.0353 | 0.890 | 0.0402 | 0.880 | 0.0450 |

(c) Ca/c=0.02

| h/c | 0.1 | | 0.5 | | 0.8 | |
|---|---|---|---|---|---|---|
| AOA(deg) | CL | CD | CL | CD | CL | CD |
| 2.5° | 0.710 | 0.0280 | 0.665 | 0.0285 | 0.636 | 0.0295 |
| 5° | 0.970 | 0.0340 | 0.860 | 0.0350 | 0.825 | 0.0360 |
| 7.5° | 1.110 | 0.0450 | 1.051 | 0.0470 | 1.017 | 0.0500 |

(d) Ca/c=0.04

It can be clearly seen that the lift coefficient is sharply grown when h/c is slightly decreased, as other parameters (camber, thickness, AOA) remaind unchanged;the reverse behavior isalso observed in the drag coefficient. Likewise, thesetrends are true when the thickness is gently lowered; whilethe reasons forthese behaviors can be explained by the contour of velocity around the airfoils for different thicknesses, which are depicted in Figs. 6(a) and (b), respectively. These figures show that the increase of thickness obviously leads to the formation of convergent–divergent passage between the airfoil and ground; consequently, it plays a significant role in the growth of velocity in the mentioned zone(Fig.7) and it is an irrefutable proof forpressure disturbance changes on the airfoil surfaces. Actually, the thickness reduction drasticallyenhances the pressure along the lower surface of airfoil and affects the pressure along the upper surface as demonstrated in Fig. 8. It can be concluded that the airfoil under the mentioned conditions causesflow blockage.

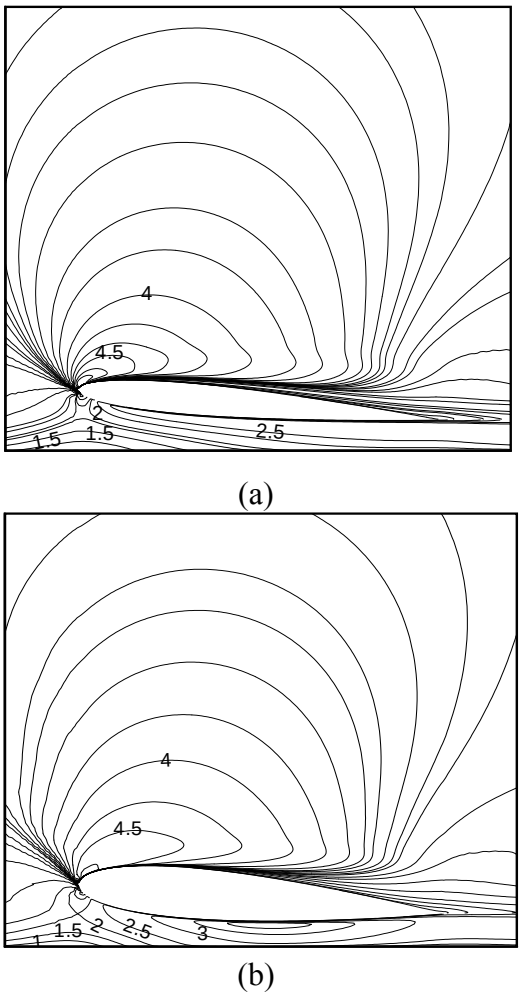


**Figure 6.** Countor of velocity around the airfoil at (a) t/c=0.09, (b) t/c=0.15 and AOA=7.5° and h/c=0.1

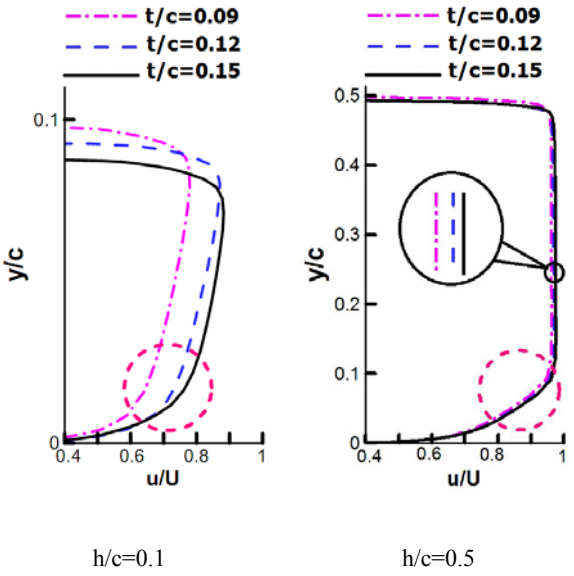


**Figure 7.** Velocity profiles between the airfoils and ground surfaces for various thickness values and AOA=5°.

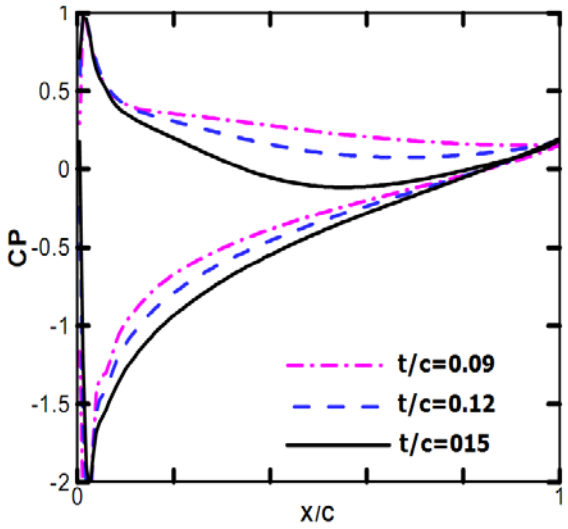


**Figure 8.** Pressure coefficient distribution on the surface of the airfoils for different thickness at AOA=5° and h/c=0.1

However, the L/D is marginally dropped in the close proximity of the ground whilethe camber of airfoil is consistently risen; but in the high ground clearance, the L/D is dramatically risen, untilit reaches a plateau and then there is a plunge, as shown in Fig.9.The trends are rooted in the air blockage in the area between the ground and the sectional wing surfaces; whenthe camber of airfoil is grown and the wing comes closer to the ground, the flow blockage would be so strong. Therefore, the thickness of the boundary layer in this area would be pressed and the lift coefficient is sharply grown (Fig.10). Nonetheless, the effect of air blockage decreases when the airfoil goes up.

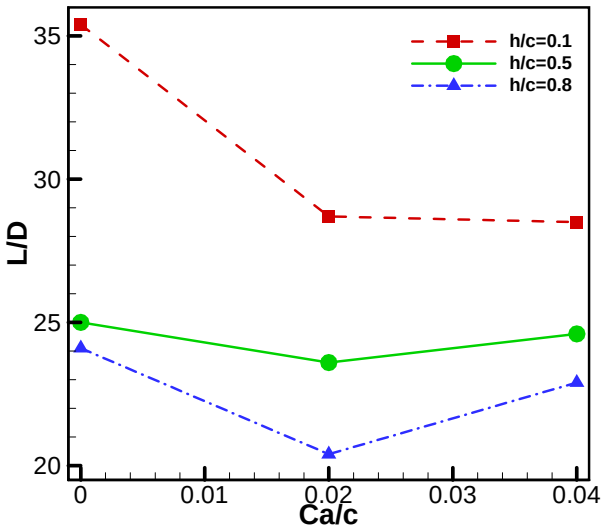


**Figure 9.** Behavior of L/D as varying camber (ca/c) and h/c for the airfoils under study.

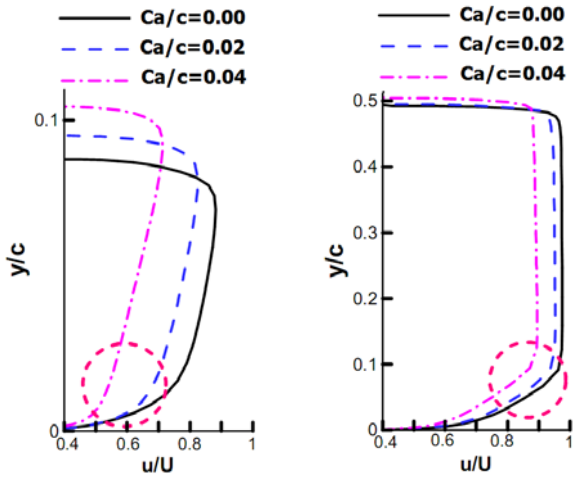


(a) h/c=0.1 (b) h/c=0.8

**Figure 10.** Velocity profile in the area between the airfoil and ground surfaces for different camber values and AOA=5°.

Hence, pressure coefficient distributions along the upper and lower surfaces of airfoils are illustrated in Fig.11 with various cambers, in both low and high ground clearances. The difference of pressure between the upper and lower surfaces is increased. Nevertheless, it is noteworthy that the pressure differences between the rtwo surfacesare enormously changed in the lower ground clearance, as can be found by the comparison between Figs. 11(a) and (b). Consequently, the lift coefficients in low h/c are significantly greaterthan in high h/c. In contrast, the drag coefficients have the reverse trend and they are slightly reduced whilethe moving airfoil approachesto the ground. On the other hand, the lift and drag coefficients have a noticeable growth by theincreasing camber; but the percentage of their growth is various. As a result, the behavior of L/D is not simplistic and easily predictable when other parameters (camber, thickness, AOA, h/c) are changed.

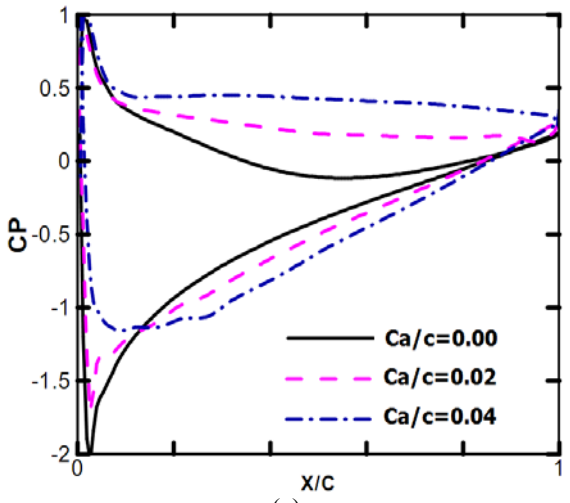


(a)

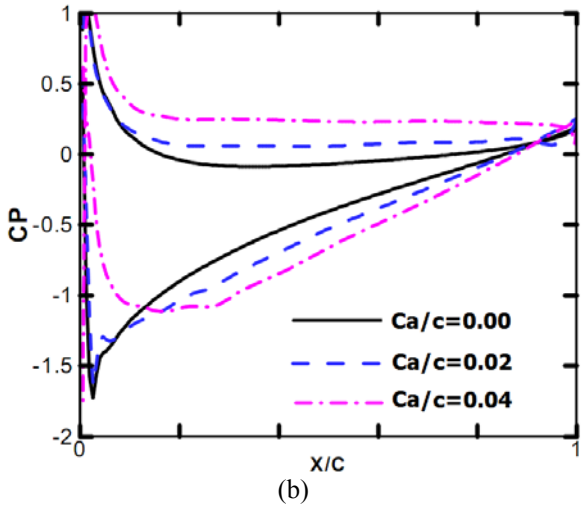


(b)

**Figure 11.** Pressure coefficient distribution on the surface of the airfoils for different cambers at AOA 5° (a) h/c=0.1, (b) h/c=0.8

As a result of the numerical simulations and above discussions, the combination of the wing shape and static conditions ompoundsthe matter of improving the performance. Actually, their relationship is nonlinear and unpredictable; thisalso sets out some powerful arguments thatboth wing shape and static conditionsshould be simultaneously deliberated in the WIG studies, especially in the optimization process. Thisis a clear illustration of the importance of using a strong and accurate optimization method.

## Optimization results

High L/D provides a net gain in economic efficiency; hence, this is one of the principal design parameters of the WIG craft. Numerical simulation makes a case for general influences of four parameters (camber, thickness, AOA, h/c) on the objective function (L/D); therefore, to find the optimum shape and condition, it is needed to go into great details. In this paper, RSM method is applied and response surface is achieved according to the numerical simulation. The data in table 2 is used to build initial response surfaces in terms of the aerodynamic coefficients and the ANFIS approach sets out some powerful rules, which will form the searching space accurately [30].

Anyway, an approximation of the optimal L/D value ($\eta_{app}$) is obtained using the active set method, which finds the global maximizer of the constructed surfaces. For the design parameters (i.e., t/c, Ca/c, h/c and AOA) yielding $\eta_{app}$, an additional numerical simulation is conducted to get $\eta_{num}$, which is compared to $\eta_{app}$. The convergence criterion in Eq. (11) decides if a new response surface is needed or not:

$$\varepsilon = \left|\frac{\eta_{num}-\eta_{app}}{\eta_{app}}\right| < 10\% \qquad (11)$$

In case a new surface is required, the interest region is systematically decreased and additional experiments are considered around the latest point found for the evaluation of $\eta_{app}$ (Fig. 1). In this study, only three additional surfaces have been constructed until convergence is reached. Fig. 12demonstrates the three response surfaces attained at the last optimization level with a final interest region range. Moreover, table 4 summarizes the main numerical results obtained during the whole optimization process. Finally, the best combination of design parameters corresponds to the aim, obtaining the maximum value of η.

Pursuant to the following sentences, the best shape characteristics of moving airfoil and static conditions are obtained by RSM, and the optimization results are presented in Table 4. According to the results, the best moving airfoil should have3.26% camber and 9.0% thickness; moreover, the optimum sectional wing should be also approximately 0.1 close to the ground and the best angle of attack is attained as over 7.5°.

**Table 4.** Optimum evolution through the optimization process

| itteration | Ca/c | t/c | h/c | AOA | L/D(Numeric) | L/D(Optimized) | error |
|---|---|---|---|---|---|---|---|
| 1 | 0.0000 | 0.090 | 0.1 | 5.54 | 32.57 | 37.12 | 0.14 |
| 2 | 0.0330 | 0.092 | 0.76 | 7.35 | 36.96 | 41.45 | 0.12 |
| 3 | 0.0326 | 0.090 | 0.1 | 7.5 | 42.01 | 45.82 | 0.09 |

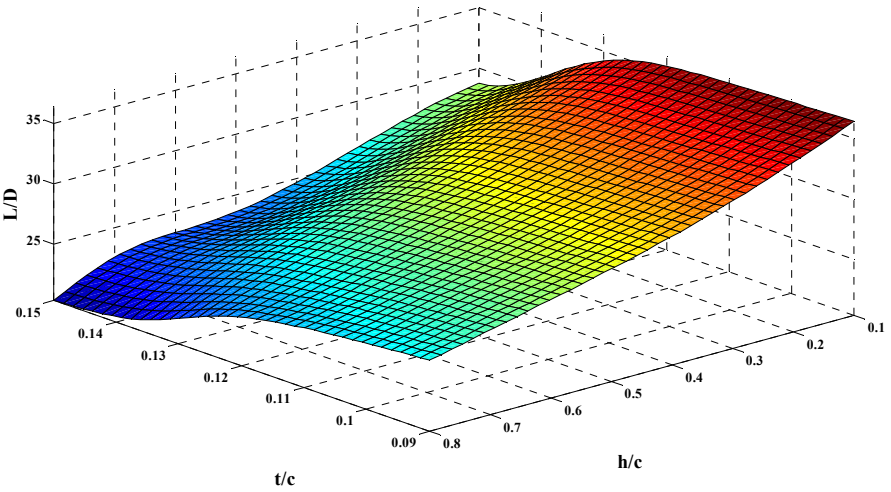


(a)

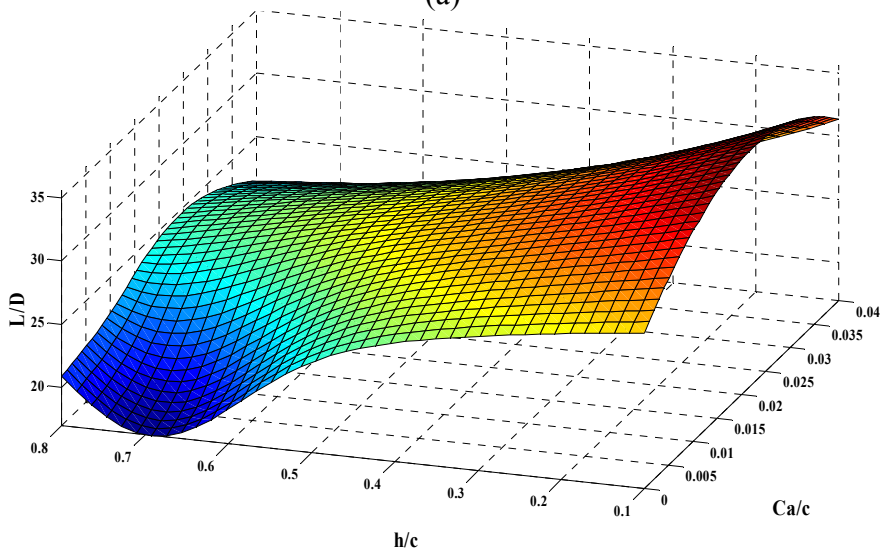


(b)

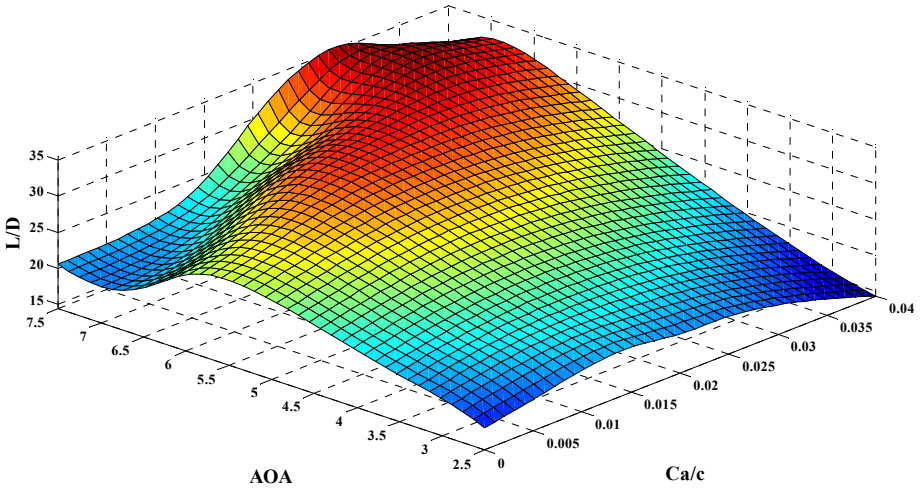


(c)

**Figure 12.** Approximated response surfaces at thethird optimization level

Furthermore, the sensitivity of design variables is computed based on the aerodynamic forces and their amount of sensitivity is depicted in Fig.13. The comparison of them explains that the lift and drag coefficients deeply depend on the angle of attack and camber from among the static conditions and wing shape parameters, respectively. Moreover, thickness of the airfoil does not have a ignificant effect on the forces; but the camber can influence them, especially the lift force. As it can be seen, the angle of attack has impressed all of the aerodynamic coefficients sharply, compared with the other effective parameters; moreover, it has dramatically influenced the CD, too. On the other hand, the ground clearance has nearlythe same effect on the drag and lift forces. Consequently, it can be said that some parameters are most impressing in the design of WIG wings and this analysis proves the fact that static conditions are very important in their optimization.Hence,the best optimum wing would be discovered when considering both shape parameters and static conditions.

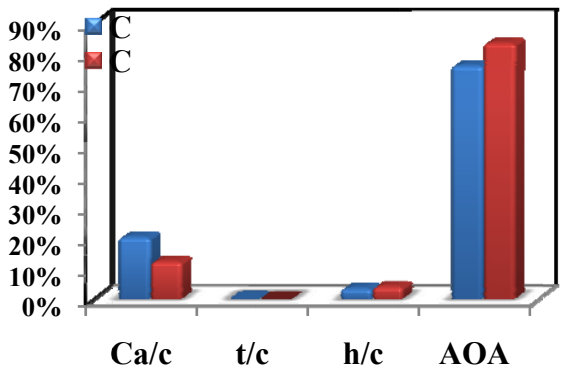


**Figure 13**. Amount of sensitivity of the design variables on the aerodynamic coefficients.

## Conclusion

The aim of this study wasto optimize the shape parameters and static conditions of a sectional wing moving close to the ground using a high order numerical procedure and response surface method (RSM). In the numerical simulation, Normalized Variable Diagram (NVD) scheme wasapplied in the boundedness criteria. Moreover, the lift to drag ratio (L/D) wasconsidered as an objective function and static conditions (ground clearance and angle of attack) and shape parameters (thickness and camber of wing) were noticeable to be considered as design variables. Adaptive Neuro-Fuzzy Interface System (ANFIS) wasemployed to generate the surface response and the amount of sensitivity of the objective function from design variables wasexplored. The results demonstrated that the best moving airfoil should have3/26% camber and 9/0% thickness; moreover, the optimum sectional wing should be also approximately 0.1 close to the ground and the best angle of attack wasattained asover 7.5°. Moreover, the thickness of airfoil didnot have a significant role on the forces; but the camber can influence them, especially the lift force. The angle of attack impressed all of the aerodynamic coefficients sharply, compared with other effective parameters; moreover, it dramatically influenced the CD, too. On the other hand, the ground clearance hadaboutthe same effect on the drag and lift forces. Consequently, it can be concludedthat some parameters are most impressing the design of WIG wings and this analysis proves this fact that static conditions are very important in their optimization.Hence the best optimum wing would be discovered when considering both shape parameters and static conditions.

## Refrences


1. Ahmed, M, Sharma S., "An investigation on the aerodynamics of a symmetrical airfoil in ground effect," *Experimental Thermal and Fluid Science*, Vol. 29, 2005, pp. 633-47.
2. Ahmed M, Ali SH, Imran, G. M, Sharma, S. D., "Experimental investigation of the flow field of a symmetrical airfoil in ground effect," *21st Applied Aerodynamics Conference*, Orlando, Florida, .2010.
3. Ahmed, M., Takasaki. T., Kohama. Y., "Experiments on the Aerodynamics of a Cambered Airfoil in Ground Effect," *44th AIAA Aerospace Sciences Meeting and Exhibit*, Reno, Nevada.
4. David JO, Jeff A., "Experimental Investigation of Various Winglet Designs for a Wing in Ground Effect," *22nd Applied Aerodynamics Conference and Exhibit. Providence*, Rhode Island, 2004, pp. 1-10.
5. Jung, K., Chun, H. and Kim. H.,"Experimental investigation of wing-in-ground effect with a NACA6409 section,"*Journal of marine science and technology,* Vol. 13, 2008, pp. 317-27.
6. Park K, Lee J.,"Influence of endplate on aerodynamic characteristics of low-aspect-ratio wing in ground effect," *Journal of mechanical science and technology*," Vol. 22, 2008, pp. 2578-89.
7. Moon Y, Oh H, Seo J., "Aerodynamic investigation of three-dimensional wings in ground effect for aero-levitation electric vehicle," Aerospace science and technology, Vol. 9, 2005, pp. 485-94.
8. Jeonghyun C, Jinsoo C, Seawook L., "Unsteady Numerical Simulation of Wings with Flapper Flying Over Nonplanar Ground Surface," *Journal of Aircraft*, Vol. 44, No. 6, 2007, pp. 1849-1855.
9. Zhang X, Zerihan J., "Aerodynamics of a double-element wing in ground effect," *AIAA Journal*, Vol. 41, 2003, pp. 1007-16.
10. Jones, B., Franke, M., Stephen, E., "Aerodynamic Ground Effects of a Tailless Chevron-Shaped UCAV Model," *American Institute of Aeronautics and Astronautics*, 1801 Alexander Bell Drive, Suite 500, Reston, VA, USA, 2006, pp. 20191-4344.
11. Djavareshkian, M. H., Esmaeili. A., Parsani, A., "Aerodynamics of smart flap under ground effect," *Aerospace Science and Technology*, Vol. 15, No. 8, 2011, pp. 642-652.
12. Nuhait A.,"Unsteady ground effects on aerodynamic coefficients of finite wings with camber," *Journal of Aircraft*, 1995, Vol. 32, pp. 186–92.
13. Djavareshkian, M. H. and Esmaeili, A., "Application of smart flap for race car wings. International," *Journal of Aerodynamics*, 2012, Vol. 2, pp. 66-92.
14. Kim Y. J., Joh C. Y., "Aerodynamic Design Optimization of Airfoils for WIG Craft Using response Surface Method," *Journal of the Korean Society for Aeronautical and Space Sciences*, Vol. 33, No. 5, 2004, pp. 18-27.
15. Kim, H.J., Chun, H .H., "Design of 2-dimensional WIG section by a nonlinear Optimization method," *Journal of Society of Naval Architects of Korea,* Vol. 35, No. 3, 1998, pp.50–59.
16. Park, K. W., Lee, J. H., "Optimal design of two-dimensional wings in ground effect using multi-objective genetic algorithm," *Ocean Engineering*, Vol. 37, 2010, pp. 902–912.
17. Lee, S. H., Lee, J. H.,; "Optimization of three-dimensional wings in ground effect using multi objective genetic algorithm," *Journal of Aircraft*, Vol. 48, No. 5, 2011, pp. 1633–1645.
18. Park K, Kim B, Lee J, Kim K., "Aerodynamics and Optimization of Airfoil Under Ground Effect," *International Journal of Mechanical Systems Science and Engineering*, Vol. 1, No. 4, 2009, pp. 385-391.
19. Lee J, Hong C, Kim B, Park K, Ahn J., Optimization of Wings in Ground Effect Using Multi-Objective Genetic Algorithm, *48th AIAA Aerospace Sciences Meeting Including the New Horizons Forum and Aerospace Exposition*, Florida, 2010.
20. Kim H, Chun H, Jung K., Aeronumeric optimal design of a wing-in-ground-effect craft. *Journal of marine science and technology*,Vol. 14, 2009, pp. 39-50.
21. Sang-Hwan Lee, Juhee Lee, 2013; Aerodynamic analysis and multi-objective optimization of wings in ground effect; Ocean Engineering, Vol. 68, No. 1, pp. 1–13.
22. Djavareshkian M.,, A new NVD scheme in pressure-based finite-volume methods. *14th Australasian Fluid Mechanics conference*, 2001, Adelaide, Australia.
23. Leonard, B.P., A survey of finite differences with upwinding for numerical modeling of the incompressible convection diffusion equation in C. Taylor and K. Morgan leds Technices in Transient and Turbulent Flow, Pineridgequess, Swansea, UK, Vol. 2, 1981, pp. 1-35.
24. Raymer D.P.,. "Enhancing Aircraft Conceptual Design Using Multidisciplinary Optimization," [PhD Thesis], *Royal Institute of Technology*, Stockholm, Sweden, 2002,.
25. Box G.E. P., Draper N.R., *Response Surfaces, Mixtures, and Ridge Analyses*, 2nd Edition, *John Wiley & Sons*, USA, 2007.
26. Haftka, R., Scott, E.P. and Cruz, J.R.,; "Optimization and experiments: a survey," *Applied Mechanics Review*, Vol. 51, No. 7, 1998, pp. 435-448.
27. Wang, G.G., Dong, Z., 2000; Design optimization of a complex mechanical system using adaptive response surface method, Transactions of the CSME, Vol. 24, No. 1B,pp. 295-306.
28. Rodriguez D.L., 2003; Response Surface Based Optimization with a Cartesian CFD Method. 41st AIAA Aerospace Sciences Meeting, Reno, Nevada, USA, 0465.
29. Bezerra, M. A., Santelli, R. E., Oliveira, E. P., Villar, L. S., & Escaleira, L. A., 2008;Response surface methodology (RSM) as a tool for optimization in analytical chemistry. Talanta, Vol. 76, No. 5, pp. 965-977.
30. Djavareshkian, M. H., Esmaeili, A., 2013; Neuro-fuzzy based approach for estimation of Hydrofoil performance. Ocean Engineering, Vol. 59, pp. 1-8.
31. Mekadem, M., Chettibi, T., Hanchi, S., Keirsbulck, L., & Labraga, L.,; Kinematic optimization of 2D plunging airfoil motion using the response surface methodology. Journal of Zhejiang University Science A, Vol. 13, No. 2, 2012, pp. 105-120.
32. Smith Justin, L., Henry, Z. G., James E Smith, "The validation of an airfoil in the ground effect regime using 2-D CFD analysis," *26th AIAA Aerodynamic Measurement Technology and Ground Testing Conference*," 2008, Reston, VA: AIAA.